Osteoarthritis and Cartilage Open 7 (2025) 100550

Contents lists available at ScienceDirect

Osteoarthritis and Cartilage Open

journal homepage: www.elsevier.com/journals/osteoarthritis-and-cartilage-open/2665-9131

MicroRNA-181a/b-1 enhances chondroprogenitor anabolism and downregulates aquaporin-9

Austin Bell-Hensley [a], Victor Gustavo Balera Brito [b], Lei Cai [b], Jin Liu [b], Kathryn Feeney [a], Hongjun Zheng [b], Audrey McAlinden [b,c,d,*]

[a] Department of Biomedical Engineering, Washington University in St. Louis, St. Louis, MO, USA
[b] Department of Orthopaedic Surgery, Washington University in St. Louis, St. Louis, MO, USA
[c] Department of Cell Biology & Physiology, Washington University in St. Louis, St. Louis, MO, USA
[d] Shriners Hospital for Children – St. Louis, St. Louis, MO, USA

ARTICLE INFO

Handling Editor: Professor H Madry

Keywords:
microRNA
miR-181a/b
Chondrogenesis
Chondrocyte
Anabolism
Aquaporin-9

ABSTRACT

Objective: Effective osteoarthritis treatments that enhance the anabolic/regenerative capacity of chondrocytes are needed. Studying cartilage development processes may inform us of approaches to control chondrocyte differentiation and anabolism and, ultimately, how to effectively treat OA. MicroRNAs are broad-acting epigenetic regulators known to affect many skeletal processes. Previous reports from our group indicated that miR-181a-1 is upregulated during chondrocyte differentiation. The goal of this study was to determine how the entire miR-181a/b-1 cluster regulates *in vitro* chondrogenesis.

Design: Precursor miR-181a/b-1 was over-expressed in cartilage progenitor cells using lentiviral technology Transduced cartilage progenitor cells were cultured as micromass pellets in hypoxic conditions and stimulated to undergo chondrogenic differentiation for five weeks. Bulk RNA-sequencing and immunostaining was applied to evaluate chondrogenic differentiation and matrix production.

Results: Immunostaining of cartilage pellet sections showed that miR-181a/b-1 increased mature type II collagen and decreased expression of the chondroprogenitor type IIA collagen isoform. Bulk RNA-Seq at day 7 of chondrogenesis revealed upregulation of pro-anabolic genes such as *COL2A1*, *COL9A2/3*, *COL11A2* and *SNORC*. Of the genes significantly downregulated by miR-181a/b-1, aquaporin 9 (*AQP9*) was the top hit which decreased in expression by over 14-fold. While a predicted target of miR-181a/b, our data showed that this miRNA cluster likely suppresses *AQP9* via an indirect targeting mechanism.

Conclusions: Our findings demonstrate a pro-differentiation/anabolic function for miR-181a/b-1 during *in vitro* chondrogenesis that may be due, in part, to suppression of *AQP9*. Future studies are needed to elucidate the role of this membrane channel protein in regulating chondrocyte differentiation and homeostasis.

1. Introduction

Osteoarthritis (OA) is a complex degenerative joint disease involving articular cartilage breakdown, often leading to pain and loss of mobility [1]. A better understanding of processes regulating cartilage development and homeostasis can provide us with important information to develop new regenerative therapies. Formation of articular cartilage tissue involves a series of complex and highly orchestrated events, as does post-natal homeostatic maintenance of mature cartilage tissue. Epigenetic control of cartilage development and homeostasis has gained interest over recent years [2,3]. Among the epigenetic regulators that have important functions in skeletal biology are microRNAs (miRNAs).

While many miRNAs have been reported to regulate cartilage development and/or homeostasis, McAlinden et al. was the first to profile miRNA expression in chondrocytes of the developing human embryonic limb [4]. Analysis of differentially expressed miRNAs revealed miR-181a-1 as significantly upregulated in hypertrophic chondrocytes, suggesting that it may regulate chondrocyte differentiation and endochondral bone formation. The gene encoding miR-181a-1 is located on chromosome 1 near the gene encoding miR-181b-1. This miR-181a/b-1

* Corresponding author. Department of Orthopaedic Surgery, Washington University in St. Louis, St. Louis, MO, USA.
E-mail addresses: aphensley@wustl.edu (A. Bell-Hensley), brito@wustl.edu (V.G.B. Brito), lei.cai@wustl.edu (L. Cai), jin.liu@wustl.edu (J. Liu), f.kathryn@wustl.edu (K. Feeney), zheng.h@wustl.edu (H. Zheng), mcalindena@wustl.edu (A. McAlinden).

https://doi.org/10.1016/j.ocarto.2024.100550
Received 15 May 2024; Accepted 21 November 2024

cluster is co-transcribed *in vivo* and processed to form the mature functional strands, miR-181a-1-5p and miR-181b-1-5p that share the same seed sequence [5,6].

To build on the miRNA profiling study by McAlinden et al. [4], Zheng et al. [7] demonstrated that over-expression of miR-181a/b-1 enhanced *in vitro* osteogenesis, in part, by increasing PI3K/AKT signaling and mitochondrial respiration. It has also been reported that injection of miR-181a-5p mimics into rodent knee joints induced a catabolic response [8] and that miR-181a-5p antagomir treatment could mitigate OA symptoms [9]. However, the function and mechanism by which miR-181a/b regulates chondrogenesis is unknown. The goal of this study was to determine how over-expression of miR-181a/b-1 in human cartilage progenitor cells (CPCs) affects chondrogenic differentiation. Utilizing TGF-β-induced CPC pellet cultures to study chondrogenesis, lentiviral-mediated miR-181a/b-1 over-expression was found to enhance anabolism, particularly type II collagen production. To gain insights into miR-181a/b-1-mediated mechanisms, bulk RNA-sequencing at day 7 of chondrogenesis demonstrated enhancement of genes and cellular pathways associated with extracellular matrix (ECM) synthesis and organization. Significant down-regulation of genes less commonly associated with chondrocyte biology were also identified. These studies provide new information on a pro-anabolic, pro--differentiation role of miR-181a/b-1 during CPC chondrogenesis. The identified transcriptomic changes induced by over-expression of this miRNA cluster lay the foundation for future avenues of research.

2. Methods

2.1. Cartilage progenitor cell isolation

Utilization of human osteoarthritic joint tissue was approved by the Washington University Human Research Protection Office (IRB ID# 201104119). Tissues were collected from six OA patients (all male, age range 54–69 yrs with no history of smoking or diabetes) who underwent knee replacement surgery at Barnes-Jewish Hospital (St. Louis, MO, USA) after obtaining informed consent. Consent details are included in the approved IRB protocol. Specimens were obtained in sterile containers within 1 h after surgery and processed immediately. Cartilage progenitor cells (CPCs) were isolated as previously described [10,11]. Briefly, cartilage pieces were diced (~1 mm^3) and digested in growth medium (DMEM/F12 with 10 % FBS, 1 % penicillin/streptomycin, 1 % amphotericin B) containing 0.025 % collagenase and 0.025 % pronase overnight at 37 °C. The resulting cell suspension was plated on a fibronectin-coated cell culture flask for 20 min. Non-adherent cells were removed, and adherent cells were trypsinized and frozen in growth medium with 10 % DMSO. CPCs were expanded up to passage 7 for experiments carried out in this study.

2.2. Lentivirus generation and transduction

Human genomic pre-miR-181a-1 (NCBI Ref Seq: NR_029626.1), pre-miR-181b-1 (NCBI Ref Seq NR_029612.1) and the intervening 61 nucleotide sequence was amplified by PCR (Table 1). The resulting miR-181a/b-1 amplicon was inserted into the pLemiR backbone (Addgene) using the Gibson Assembly Master Mix (New England Biolabs). Stocks of pLemir lentivirus expressing pre-miR-181a/b-1 (LV-181) or a non-silencing (NS) control RNA (LV-NS) [12] were prepared as previously described [7,11] and titered using the Lenti-X™ qRT-PCR Titration Kit (Takara Bio USA) according to the manufacturer's instructions. Aliquots of lentivirus stocks were stored at −80 °C and used within two freeze-thaw cycles. Passage 7 CPCs were transduced with LV-181 or LV-NS in growth medium containing 100 μg/mL protamine sulfate. Transduced CPCs were cultured for 3 days prior to pellet formation. Cell viability was assessed using brightfield microscopy.

2.3. Chondrogenic differentiation assay

Transduced CPCs were trypsinized and resuspended in chondrogenic induction medium [serum-free high glucose DMEM containing TGF-β3 (10 ng/mL), 1 % ITS+, dexamethasone (100 nM), ascorbate (100 μM), L-proline (40 μg/mL)] [13]. Cells were seeded in 15 mL conical tubes (3×10^5 cells/tube) and centrifuged at 300×*g* for 5 min. Chondrogenic induction media was refreshed three times per week for five weeks. CPC pellets were incubated at 37 °C in 5 % O_2 for the duration of the assay. Non-transduced CPC pellets were used as controls.

2.4. RNA isolation

On days 7 and 35 of chondrogenesis, pellets were collected for RNA isolation. Pellets were pooled to collect sufficient RNA for RNA-sequencing and qPCR (day 7; 8–10 pellets) or just qPCR (day 35; 2–4 pellets). Pooled pellets were suspended in lysis buffer from Norgen Bio-Tek's Total RNA Purification kit for 5 min, then flash frozen in liquid nitrogen. Frozen pellets were dissociated using a motorized pellet pestle (DWK Life Sciences GmbH). RNA was extracted using Norgen BioTek's Total RNA Purification kit according to the manufacturer's instructions. Total RNA was quantified using a NanoDrop 2000 Spectrophotometer (Thermo Fisher) then stored at −80 °C.

2.5. Quantitative polymerase chain reaction

To quantify miR-181a-5p and miR-181b-5p, a TaqMan microRNA reverse transcription kit, TaqMan master mix with no UNG and TaqMan primer/probe sets (Life Technologies Inc; Table 1) were used [11]. To

Table 1
Primer sequences and Life Technologies miRNA assay IDs used for vector cloning and quantitative PCR. Bolded sequence indicates miR-181a/b-5p binding site. Bolded and italicized sequence indicates mutated sequence within miR-181a/b-5p binding site.

Amplicon	Forward Primer	Reverse Primer
miR-181-a/b-1	CTGGGGCACAGATAACCAATGTGA	AGGGGCGGAATTTGCTACAACAGT
Genomic	TGTGGAGGTTTG	AGGAAGGTG
miR-181a-5p	TaqMan miRNA assay ID 000480 (Life Technologies Inc.)	
miR-181b-5p	TaqMan miRNA assay ID 001098 (Life Technologies Inc.)	
RNU44	TaqMan miRNA assay ID 001094 (Life Technologies Inc.)	
PPIA	TCCTGGCATCTTGTCCATG	CCATCCAACCACTCAGTCTTG
COL2A1	GGCAATAGCAGGTTCACGTACA	CGATAACAGTCTTGCCCCACTT
AQP9	GTGAGGACCACAACAGGTAGG	GCCACATCCAAGGACAATCAAG
AQP9 3′-UTR	CTAGCGGGAAGATAAGTTGAGTTG	TCGACAGCCAGCTACTGATCTTCT
WT	TCCAAGAGCACACTGAAAGT**TGAA**	GAAAGGTAGAGGAATGCATTAGAT
	TGTTATCTAATGCATTCCTCTACCTT	A**ACATTCA**ACTTTCAGTGTGCTCT
	TCAGAAGATCAGTAGCTGGCTG	TGGACAACTCAACTTATCTTCCCG
AQP9 3′-UTR	CTAGCGGGAAGATAAGTTGAGTTG	TCGACAGCCAGCTACTGATCTTCT
MUT	TCCAAGAGCACACTGAAAGT**TACC**	GAAAGGTAGAGGAATGCATTAGAT
	TGTTATCTAATGCATTCCTCTACCTT	A**ACAGGTA**ACTTTCAGTGTGCTCT
	TCAGAAGATCAGTAGCTGGCTG	TGGACAACTCAACTTATCTTCCCG

measure mRNAs, reverse transcription using Superscript RT II (Life Technologies Inc.) and qPCR was performed using PowerUp SYBR master mix (Life Technologies Inc.). PCR primer sequences are shown in Table 1. Fold changes were calculated using the $2^{-\Delta Ct}$ method using RNU44 as a reference small RNA or *PPIA* as a reference mRNA.

2.6. Histology and immunofluorescence

Pellets (day 35) were fixed in 10 % neutral-buffered formalin, embedded in paraffin, sectioned (10 μm) and mounted on glass histology slides. Safranin-O staining was carried out on deparaffinized slides with Weigert's Hematoxylin (1.5 min), 0.2 % Fast Green (2 min), and 0.1 % Safranin O (6 min). Samples were dehydrated and coverslipped using CytoSeal XYL (Thermo Fisher). For immunofluorescent staining, deparaffinized sections were treated with Proteinase K (10 μg/mL in 10 mM Tris-HCl, pH 7.5) for 20 min at 37 °C (COLII and COLIIA) or sodium citrate (10 mM in 0.05 % Tween 20, pH 6.0) for 10 min at 90 °C (AQP9). Sections were rinsed, blocked, then incubated overnight at 4 °C with the following primary antibodies: COLII (1:200 dilution; a gift from Dr. David Eyre, University of Washington, Seattle), COLIIA [14] (1:200 dilution; a gift from Dr. Linda Sandell, Washington University, St. Louis), aquaporin 9 (AQP9) [15] (1:50 or 1:200 dilution; Alpha Diagnostics International Cat. No. #AQP91-A). Sections were incubated with species-specific secondary antibodies (1:200 or 1:400 dilution) conjugated to Alexa fluorescent dyes (Invitrogen: goat anti-rabbit Alexa 488; goat anti-rat Alexa 594) for 1 h at room temperature. Sections were rinsed and coverslipped using DAPI mounting medium (Electron Microscopy Sciences). Brightfield and fluorescent images were taken on a whole slide imaging system (Hamamatsu Photonics Nanozoomer 2.0-HT System) using a 20X magnification lens or an inverted confocal microscope (Leica DMi8) using a 63X magnification lens.

2.7. Quantitative assessment of histology and immunofluorescence images

Images of the Safranin-O and immunostained pellet tissue sections were imported into ImageJ software for analysis. Total cross-sectional area was quantified by converting the Safranin-O staining to an 8-bit image and using the ImageJ "Threshold" tool. Positive staining area for Safranin-O, COLII, COLIIA, and AQP9 slides were quantified using appropriate color thresholds for each stain, and the positive area was divided by the total area to obtain an area fraction.

2.8. Bulk RNA sequencing and pathway analysis

RNA isolated from day 7 chondrogenic pellets (LV-NS, LV-181; $n = 4$ different donors) were submitted for bulk RNA-Sequencing (RNA-Seq). Libraries were prepared according to manufacturer's protocol, indexed, pooled, and sequenced on an Illumina NovaSeq X Plus. Basecalling and demultiplexing were performed with DRAGEN and BCLconvert v4.2.4. Reads were aligned to the Ensembl release 101 with STAR v2.7.9a [16], and counts were derived from uniquely aligned unambiguous reads using Subread:featureCount v2.0.3 [17]. Counts were imported into EdgeR [18] for TMM normalization to adjust for library size. Using Limma [19], weighted likelihoods based on the mean-variance relationship were calculated, and log 2 counts-per-million were determined using voomWithQualityWeights [20] for differential expression analysis. Genes with a Benjamini-Hochberg adjusted p-values $\leq$0.05 were considered significant. Global perturbations in Gene Ontology (GO) terms, MSigDB Reactome pathways and MSigDB microRNA target gene sets (miRDB v6.0) were analyzed using GAGE [21]. Raw and processed data has been uploaded to the GEO depository (GSE262978).

2.9. MicroRNA target prediction

A search for predicted miR-181a/b-5p target mRNAs was performed using the TargetScan database (http://www.targetscan.org/) [22] and the miRanda algorithm [23].

2.10. Luciferase assay

Human AQP9 3′-UTR wild-type (WT) and mutated (MUT) oligonucleotide sequences (Table 1) were cloned into the pmirGLO Dual-Luciferase miRNA Target Expression Vector (Promega). Given that TNF-α is a known target of miR-181a [24], plasmid pmirGLO-3′UTR-TNF (Addgene #153069) containing the human TNF-α 3′UTR sequence downstream of the luciferase reporter gene was used as a positive control. Plasmids were transfected into human embryonic kidney (HEK293) cells, then cells were transduced with LV-181 or LV-NS. Cells were incubated at 37 °C for 48 h, then luciferase activity was assessed with the Dual-Glo® Luciferase Assay System (Promega) according to the manufacturer's instructions on an Agilent BioTek Cytation 5 microplate reader.

2.11. Statistical analysis

All experiments were carried out in triplicate with CPCs from 3 to 4 independent biological donors. Data are presented as mean ± SD and statistical comparisons were made using paired t-tests with pairing between CPCs from the same donor, except for RNA expression data which was compared using ratio paired t-tests to better assess proportional differences. Probability values were considered statistically significant at $p \leq 0.05$.

3. Results

3.1. miR-181a/b-1 over-expression promotes chondrogenic differentiation

The ECM of chondrogenic pellet tissue sections was examined to assess the effects of lentiviral-mediated over-expression of miR-181a/b-1 (LV-181) compared to non-silencing RNA (LV-NS). Quantitative analysis of Safranin-O-stained tissue sections showed a trend toward increased staining intensity indicating higher levels of proteoglycan synthesis (Fig. 1A–C; Supp. Fig. 1). Collagen composition was evaluated by immunolocalization of mature type II collagen fibers and type IIA procollagen, the COL2A1 isoform expressed by chondroprogenitor cells [25]. Analysis of immunostained images showed a significant increase in COLII positive area fraction in the LV-181 group (COLII; Fig. 1D–F; Supp. Fig. 2). Conversely, there was a trend toward decreased COLIIA positive area in LV-181 pellets compared to LV-NS (COLIIA; Fig. 1G–I; Supp. Fig. 3). Over-expression of functional miR-181a/b-5p was confirmed in the LV-181 group compared to LV-NS at day 7 and day 35 (Fig. 1J and K). There was a significant decrease in miRNA expression over time in the LV-181 group which is expected in these viral transduced cultures. At day 35, there is still significant over-expression of the miR-181a/b. At day 7 and day 35, *COL2A1* gene expression levels were significantly increased in the LV-181 group (Fig. 1L) which agrees with enhancement of type II collagen at the protein level (Fig. 1D–F). In summary, miR-181a/b-1 over-expression appeared to promote chondrocyte differentiation as indicated by enhanced type II collagen gene and protein expression, and reduction of the "chondroprogenitor" type IIA collagen isoform.

3.2. miR-181a/b-1 over-expression promotes cartilage anabolism

To determine the mechanism by which miR-181a/b-1 modulates chondrogenesis, bulk RNA-Seq and pathway analysis were carried out on day 7 RNA samples. Principal component analysis (PCA) shows separation of LV-NS and LV-181 samples with higher variability between samples of the LV-181 group (Fig. 2B). We identified 75 significantly differentially expressed genes with a Benjamini-Hochberg adjusted FDR p-value $\leq$0.05 and Log_2(Fold Change) $\geq$ 2 (Fig. 2B; Supp. Table 1). Among the most significantly upregulated genes were several markers associated with the mature chondrocyte phenotype and cartilage anabolism including *COL2A1*, *COL9A2/3*, *SNORC*, *COL11A2*, *MATN4*, and *CSPG4*. Analysis of *COL2A1* expression via

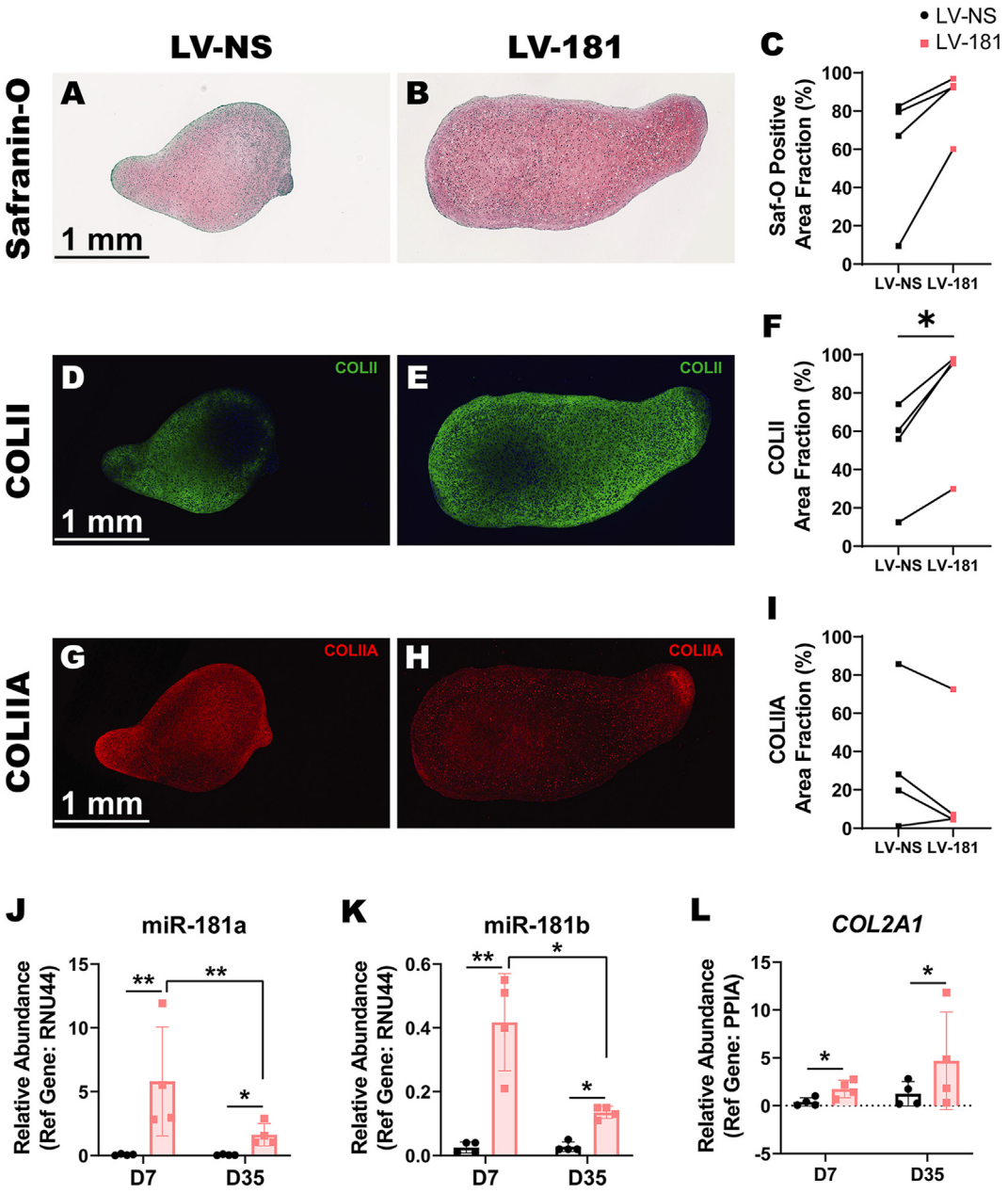

Fig. 1. Chondrogenic differentiation enhanced by miR-181a/b-1 over-expression. A-I) Representative images and quantitative analysis of Safranin-O histology (Saf-O; **A-C**), immunostaining for type II collagen (COLII; **D-F**), and type IIA pro-collagen (COLIIA; **G-I**) in pellet cultures after 35 days of chondrogenic induction. Positive staining was quantified as a percentage of the total cross-sectional area for quantitative analyses (**C, F, I**). Comparison between NS *vs.* 181; $*p < 0.05$, $n = 4$ CPC lines from independent donors. For histology and immunostaining, each dot represents the average from 3 to 4 pellets derived from CPCs of a single donor. **J-L)** Relative abundance of miR-181a-5p (**J**), miR-181b-5p (**K**), and type II collagen (*COL2A1*) (**L**) expression following lentiviral overexpression of the miR-181a/b-1 cluster after 7 and 35 days. Comparisons between NS *vs.* 181, and day 7 *vs.* 35; $*p \leq 0.05$. $n = 4$ CPC lines from independent donors. RNA was pooled from 7 to 10 pellets (Day 7) or 2–4 pellets (Day 35). Abbreviations: LV-NS, lentivirus encoding non-silencing miRNA sequence; LV-181, lentivirus encoding pre-miR-181a/b-1; Saf-O, Safranin-O; COLII, type II collagen; COLIIA, type IIA pro-collagen. Histology and immunostaining images for all pellets are available in Supp. Fig. 1 (Saf-O), Supp. Fig. 2 (COLII), and Supp. Fig. 3 (COLIIA).

qPCR at day 7 (Fig. 1L) also showed enhanced expression in the LV-181 group which agreed with the RNA-Seq data. GO biological processes upregulated by LV-181 included cartilage anabolic pathways such as *skeletal system development* and *extracellular structure organization* (Fig. 2C; Supp. Table 1). Reactome biological pathways upregulated in the LV-181 group included *collagen biosynthesis and modifying enzymes*, *collagen formation*, and *collagen chain trimerization* (Fig. 2D; Supp. Table 1). These findings support a role for miR-181a/b-1 in promoting cartilage anabolism and ECM formation, particularly collagen II synthesis.

3.3. *miR-181a/b-1 downregulates potential target genes*

RNA-Seq also revealed many significantly down-regulated genes in response to miR-181a/b-1 over-expression during chondrogenesis (Fig. 2A; Supp. Table 1). This was further evidenced by GAGE analysis using the miRDB microRNA target gene set, which identified miR-181 predicted targets among the top enriched down-regulated sets (Supp. Fig. 4). Some of these down-regulated genes were confirmed direct targets of miR-181a/b, such as *CBX7* [26] and *TGFBR1* [27]. MiRanda [23] was used to score miRNA-mRNA interactions for all protein-coding

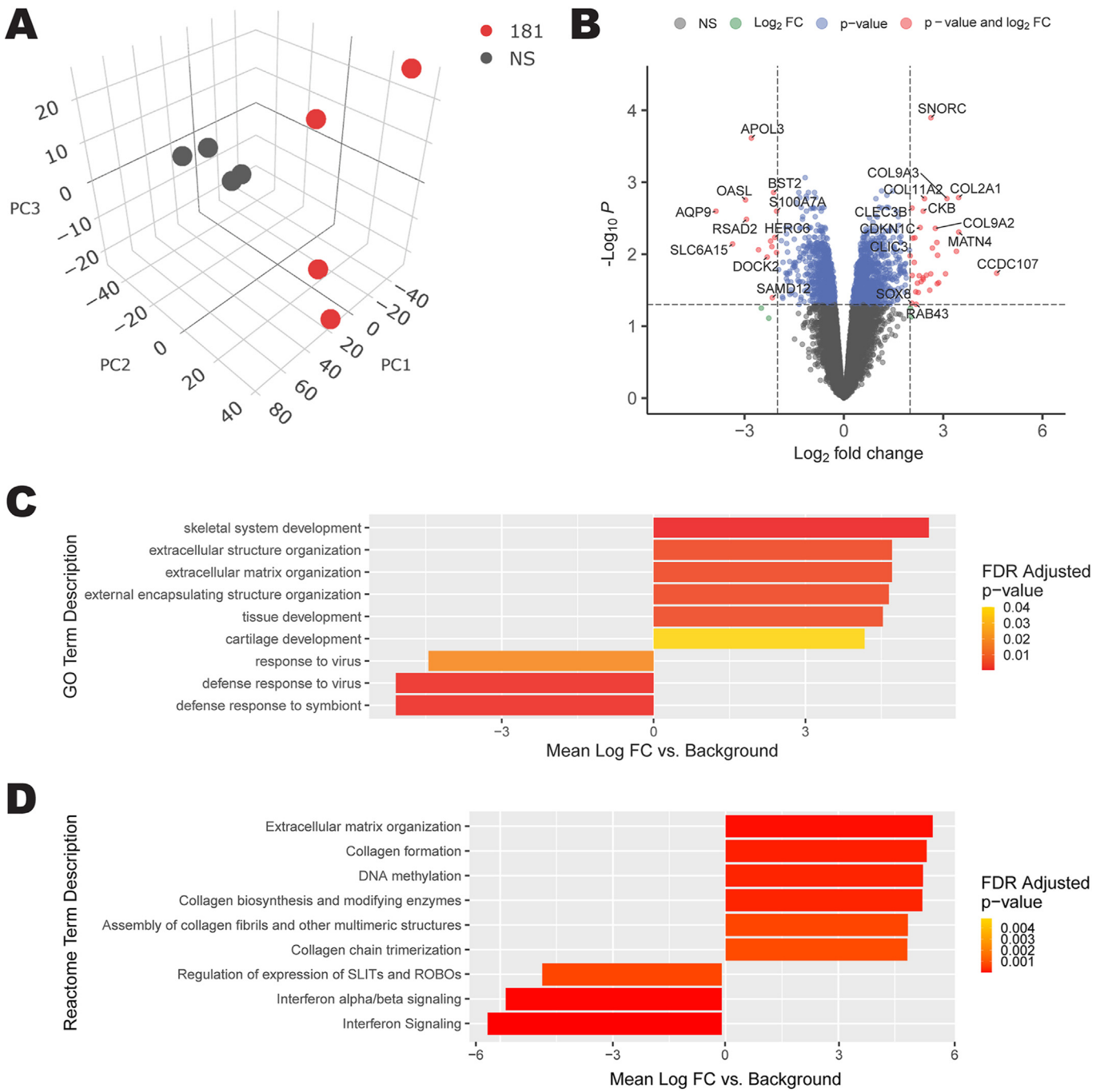

Fig. 2. Differentially expressed genes following miR-181a/b-1 over-expression. A) Principal Component Analysis (PCA) plot showing transcriptome variability across all samples. **B)** Volcano plot showing differentially expressed genes in CPCs after 7 days of chondrogenic induction following miR-181a/b-1 overexpression. *P*-values are adjusted using the Benjamini-Hochberg false discovery rate. Top significantly perturbed GO biological processes (**C**) or perturbed Reactome biological pathways (**D**) at Day 7 of CPC chondrogenesis following miR-181a/b-1 overexpression. For the full list of differentially expressed genes and enrichment analysis, refer to Supp. Table 1.

genes detected in the RNA-Seq readout (Fig. 3A), with a miRNA target prediction threshold score of ≥140 [28]. Several targets of miR-181a/b-5p that have been confirmed *in vitro* generated MiRanda scores ≥140 with *TGFBR1* being the highest with a score of 147. The top significantly downregulated gene from our RNA-Seq analysis was aquaporin-9 (*AQP9;* 14.54-fold decrease; $p = 2.5E\text{-}03$) (Fig. 2A; Supp. Table 1). Interestingly, *AQP9* had a MiRanda score of 161 for miR-181a/b-5p (Fig. 3A). These findings suggest that *AQP9* may be a direct target of this miRNA cluster.

3.4. *AQP9 is an indirect target of mir-181a/b-1*

To determine if miR-181a/b-5p directly targets *AQP9*, a dual luciferase reporter assay was carried out using plasmids containing the wild-type (WT) 3′UTR of *AQP9* or a or mutant (MUT) plasmid containing mutations in the predicted miR-181a/b binding site in the 3′UTR of *AQP9* (Fig. 3B). As a positive control, miR-181a/b binding to a known target sequence in the 3′UTR of TNF-α was also tested. We found that relative luminosity was unchanged by LV-181 treatment in cells transfected with

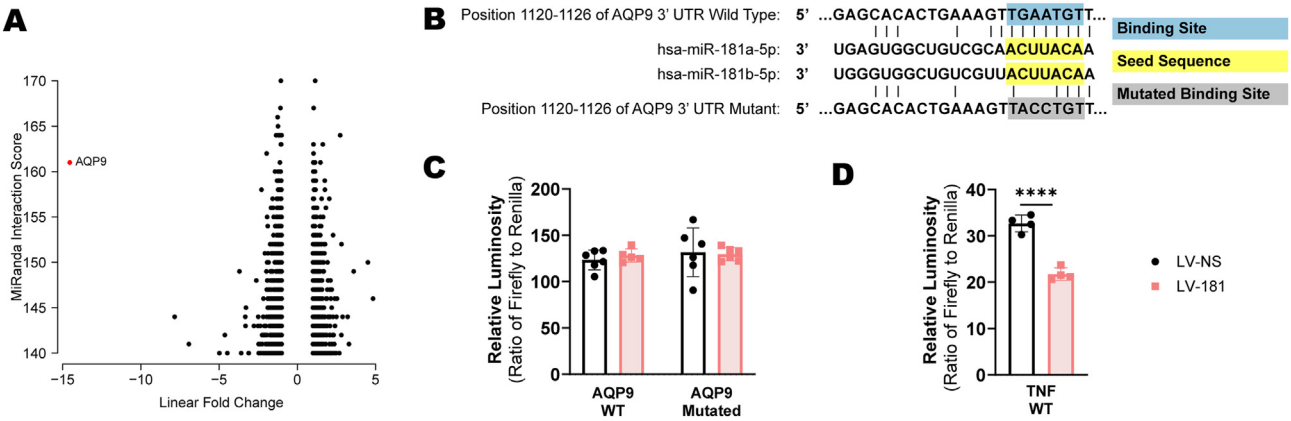

Fig. 3. Aquaporin-9 is not a direct target of miR-181a/b-1. **A**) Predicted targets of miR-181a/b-5p based on MiRanda interaction scoring algorithm compared to their linear fold change. **B**) Sequence of human wild-type (WT) AQP9 3′UTR containing the predicted miR-181a/b binding site (blue), and the mutated (MUT) miR-181a/b binding site in the AQP9 3′UTR (grey). Seed sequence of miR-181a/b-5p is shown in yellow. For the luciferase assays, plasmids containing WT and MUT 3′UTR of AQP9 were transfected in HEK cells. **C**) Relative luminosity in HEK cells transduced with LV-NS or LV-181 together with WT or MUT AQP9 3′UTR-containing reporter plasmids. **D**) Relative luminosity in HEK cells transduced with LV-NS or LV-181 together with the reporter plasmid containing WT TNF-α 3′UTR as a positive control. Comparisons between NS *vs.* 181, and WT *vs.* MUT; $n = 4$, $^{****}p < 0.0001$. (For interpretation of the references to colour in this figure legend, the reader is referred to the Web version of this article.)

AQP9 3′UTR WT or MUT plasmids (Fig. 3C) while there was a significant decrease in luminosity in LV-181 transduced cells containing the TNF-α 3′UTR plasmid, as expected (Fig. 3D) [24]. This indicates that *AQP9* is an indirect target of miR-181a/b.

3.5. *AQP9* expression is downregulated during chondrogenic differentiation

We carried out RT-qPCR to confirm the indirect downregulation of *AQP9* by miR-181a/b-1 over-expression at both day 7 and day 35 of chondrogenesis (Fig. 4A). Evaluation of *AQP9* baseline expression in the LV-NS group showed a trend toward decreased *AQP9* expression at day 35 of chondrogenesis compared to day 7 (Fig. 4A). Statistical significance was not reached due to one outlier with endogenously low *AQP9* expression. We also evaluated a publicly available bulk RNA-Seq dataset from Huynh et al. describing the transcriptome of MSCs during chondrogenesis (GEO accession: GSE109503) [29]. The chondrogenic assay performed by Huynh et al. used the same chondrogenic medium, but a different progenitor cell source (passage 4 human MSCs), and 20 % O_2 culture conditions. Despite these differences, they showed higher *AQP9* expression from day 0 to day 3 which decreased to negligible levels by day 21 (Fig. 4B). Taken together, it appears that *AQP9* expression decreases during *in vitro* chondrogenesis. Additionally, our studies show that miR-181a/b-1 further suppresses *AQP9* during chondrogenesis, but likely not due to a direct targeting mechanism.

3.6. Aquaporin-9 protein expression in chondrogenic cells

We carried out immunolocalization of AQP9 protein in cells of day 35 CPC-derived chondrogenic pellet tissue sections. As a positive control, we stained tissue from murine (C57BL/6) liver tissue since AQP9 is highly expressed in the plasma membrane of hepatocytes [30]. As expected, robust AQP9 expression was observed at the cell membrane of liver cells (Fig. 5A). However, fluorescent staining patterns in tissue sections from day 35 non-transduced chondrogenic pellets revealed mostly intracellular staining (Fig. 5B). AQP9 immunolocalization was also carried out in monolayer human CPCs and primary chondrocytes, and intracellular staining was also observed whether cultured in hypoxic (5 % O_2) or normoxic (20 % O_2) conditions (Supp. Fig. 5). Comparing AQP9 expression in cells from LV-NS and LV-181 pellets also revealed

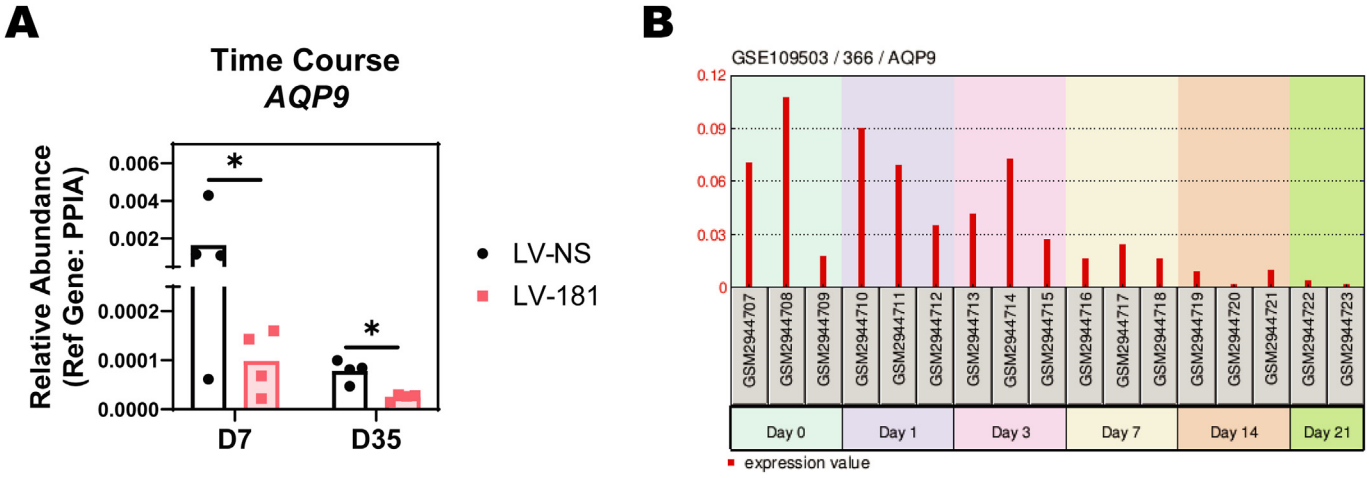

Fig. 4. Aquaporin-9 is downregulated by miR-181a/b-1 over-expression. **A**) qPCR analysis of *AQP9* expression at days 7 and 35 of chondrogenic induction. Comparisons between NS *vs.* 181, and day 7 *vs.* 35; $^{*}p < 0.05$. $n = 4$ CPC lines from independent donors. For each CPC line, RNA was pooled from 7 to 10 pellets (Day 7) or 2–4 pellets (Day 35). **B**) Expression pattern of *AQP9* in human MSC chondrogenesis (Data retrieved from GEO accession GSE109503).

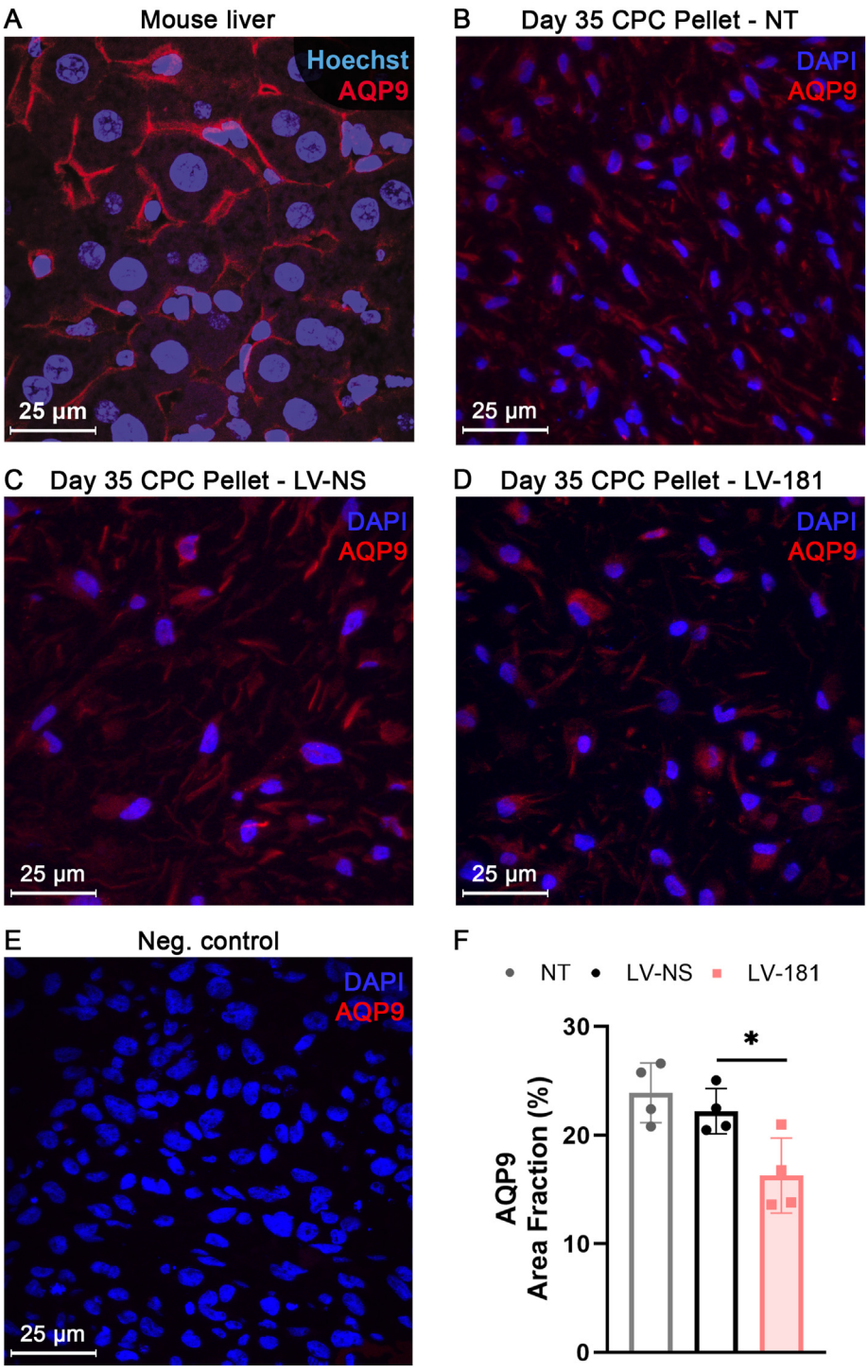

Fig. 5. Localization of aquaporin-9 protein in chondrogenic cells. A-F) Immunostaining of aquaporin-9 (AQP9) in (**A**) mouse liver tissue from a wild-type C57BL/6 mouse (positive control), (**B**) Non-transduced (NT) CPC pellet tissue; (**C**) LV–NS–transfected CPCs pellet tissue and (**D**) LV-181-transfected CPC pellet tissues after 35 days of chondrogenic induction, (**E**) immunostaining negative control in LV-NS pellet tissue sections, and (**F**) Quantitative analysis of AQP9 immunostaining. Positive staining was quantified as a percentage of the total area. Comparisons between NT *vs.* NS, and NS *vs.* 181; $*p < 0.05$, $n = 4$ CPC lines from independent donors.

intracellular staining while no signal was observed in control (no primary antibody) sections (Fig. 5C–E). Attempts to quantify AQP9 staining revealed lower levels of expression in cells from LV-181 pellets compared to the LV-NS group (Fig. 5F) which agrees with our findings at the gene expression level.

4. Discussion

We report that the miR-181a/b-1 cluster promotes anabolic pathways in TGF-β-induced chondrogenic differentiation of CPCs in pellet cultures under hypoxic conditions *in vitro*. CPCs are a well-described cell source to study chondrogenesis [31]. Hypoxic condition was chosen to recapitulate the low oxygen environment experienced by chondrocytes *in vivo* and have been used by others in the field [13,31,32].

Anabolic effects of miR-181a/b-1 over-expression were evident from some of the top upregulated genes identified from RNA-Seq including *SNORC*, *MATN4*, and *CKB* which are expressed in articular and/or growth plate chondrocytes and regulate chondrocyte differentiation and/or ECM homeostasis [33–35]. Upregulation of these genes in addition to *COL2A1*, *COL9A2/3,* and *COL11A2* suggest a pro-anabolic, pro-differentiation role for miR-181a/b-1 during CPC chondrogenesis. This is further supported by the significantly upregulated GO and Reactome

pathways that included ECM organization and collagen synthesis, assembly and trimerization (Fig. 2). There are mixed reports in the published literature on effects of miR-181 homologs on collagen synthesis. In our system, the multi-functional effects of miR-181a/b may activate collagen gene transcription. Reports show that miR-181a/b can alter cell metabolism [7,36]. While the top modified pathways in our studies do not suggest a major shift in metabolic processes, we cannot rule out potential subtle changes in metabolites that may enhance the ability of the cells to differentiate and synthesize/secrete collagen. Future epigenetic and metabolomics-based studies may help elucidate how miR-181a/b enhances collagen and ECM synthesis.

In addition to pro-anabolic effects, over-expression of miR-181a/b-1 also appeared to suppress catabolic processes as indicated by downregulation of a number of Reactome pathways including *IL-1 signaling*, *TNFR2 non-canonical NF-kB pathway*, and *cytokine signaling in immune system* (Supp. Table 1). Anti-inflammatory functions for miR-181a/b have been reported in the published literature [24,37]. Dampening of catabolic events during TGF-β-induced chondrogenesis may also explain why anabolism is higher in the LV-181 group. Other top downregulated GO and Reactome pathways were related to interferon (IFN) signaling. While this may suggest that batches of LV-181 induced a more robust anti-viral response in cells compared to LV-NS titers, there are reports that IFN signaling suppresses *in vitro* chondrogenesis [38]. Therefore, suppression of IFN pathways may be another mechanism by which miR-181a/b-1 enhances chondrogenesis.

With respect to miR-181a/b effects on cartilage homeostasis, Nakamura et al. demonstrated that intra-articular injection of miR-181a mimics in a rat model of spinal facet joint OA exacerbated NF-κB mediated cartilage catabolism and degradation [8]. The same group showed that intra-articular injections of miR-181a antagomirs protected against cartilage degradation in a rat model of facet joint OA and a mouse model of trauma-induced knee OA [9]. Another study reported that miR-181b may induce OA progression in rats [39]. These *in vivo* studies examined the effects of miR-181a/b in mature cartilage tissue which is different from the goals of this study where we determined effects on chondro-progenitor cell differentiation. It may be that miR-181 homologs induce different effects depending on cell differentiation status. While it may induce catabolism in mature chondrocytes *in vivo*, our results point to an anabolic effect during TGF-β-induced chondrogenesis *in vitro* and highlights the complexities of miRNA function. Generation of a miR-181a/b-1 knock-in mouse model could be useful to study effects of overexpression on *in vivo* cartilage development. In support of our findings, one study reported decreased MSC chondrogenesis by miR-181a antagomir treatment [40]. While we did not pursue antagomir approaches in these studies, it will be interesting to test effects of inhibiting different miR-181 family members on chondrogenic differentiation.

Our previous miRNA profiling study [4] revealed higher expression of miR-181a-1 in hypertrophic chondrocytes compared to less differentiated chondrocytes of the developing human growth plate. Gabler et al. [41] reported a correlation between miR-181a expression and the hypertrophic chondrocyte marker *COL10A1* during *in vitro* MSC chondrogenesis. We also found increased baseline expression of miR-181a/b during CPC chondrogenesis (Supp. Fig. 6). However, we did not detect type X collagen staining in day 35 chondrogenic pellets, which is not surprising given CPCs are derived from articular cartilage and have a low tendency toward hypertrophy [31]. Over-expression of miR-181a/b did not promote CPC hypertrophy, but perhaps a differentiation assay longer than 35 days would be required to see effects. We chose CPCs as our progenitor source due to our experience of achieving higher success rates of chondrogenic induction with these cells when compared to using BMSCs. Taken together, while we report a pro-anabolic/pro-differentiation role for miR-181a/b-1, its potential function in inducing hypertrophic differentiation cannot be addressed in these studies.

Examination of the genes significantly down-regulated by miR-181a/b-1 revealed an enrichment in potential direct targets of this miRNA cluster (Supp. Fig. 4). Of these, *CBX7* (chromobox 7) was identified as direct target of miR-181a/b [26]. This study by O'Loghlen et al. [26], showed that miR-181-mediated suppression of *CBX7* resulted in enhanced embryonic stem cell differentiation. It will be interesting in future studies to explore the role of CBX7/miR-181a/b axis in regulating progenitor cell differentiation toward the chondrocyte lineage. The top significantly downregulated gene, *AQP9*, is also a predicted target of miR-181a/b. The miRNA binding site is not evolutionarily conserved and only present in the 3′UTR of human *AQP9*. Our studies did not confirm *AQP9* as a direct target of miR-181a/b. Further studies are needed to determine how this miRNA cluster indirectly suppresses AQP9.

Very little is known about AQP9, or any of the other 12 identified aquaporins, in skeletal tissues. Aquaporins are transmembrane channels essential for regulating water, energy and redox homeostasis in cells [42]. AQP9 is an aquaglycerporin that transports water, glycerol, urea and hydrogen peroxide [43]. Examining AQP9 protein localization in chondrogenic cells revealed intracellular staining patterns when compared to primarily plasma membrane localization in liver cells. Intracellular staining has also been observed in chondrocytes from OA articular cartilage [44]. While aquaporins are most commonly expressed on the plasma membrane, there is evidence for expression in the membrane of the endoplasmic reticulum and lysosomes [45,46]. AQP9 has also been found to be expressed on the inner mitochondrial membrane [15]. Future studies are needed to clarify the exact location of AQP9 in chondrocytes.

There are only a few published studies on AQP9 in skeletal cells. Aharon et al. demonstrated that treatment with phloretin, a non-specific AQP9 inhibitor, suppressed osteoclast differentiation, specifically in the fusion process [47]. However, analysis of *AQP9*$^{-/-}$ mice demonstrated that AQP9 was not necessary for osteoclast differentiation *in vitro* or *in vivo* [48]. Contradictory studies in AQP9 null mice revealed attenuation of bone loss induced by microgravity due to inhibition of osteoclastogenesis [49]. With regards to cartilage development, analysis of growth plates from AQP9$^{-/-}$ mice revealed a thicker proliferating zone [50]. Studies in human chondrocyte cultures showed that downregulation of AQP9 decreased the catabolic response to IL-1β and that levels of AQP9 protein were higher in chondrocytes from OA patients [44]. These studies suggest that AQP9 may inhibit chondrocyte proliferation during development and enhance catabolic responses in primary chondrocytes. In this context, our observation that AQP9 levels decrease during CPC chondrogenesis makes sense as does the fact that miR-181a/b further suppressed AQP9. More studies are needed to fully understand the role of AQP9 during cartilage development and it will be interesting to assess if the absence of AQP9 in mice confers higher resistance to OA development.

Author contributions

Conception and design: ABH, HZ, VGBB, LC, AM. Analysis and interpretation of the data: ABH, HZ, VGBB, LC, AM. Drafting of the article: ABH, VGBB, AM. Critical revision of the article for important intellectual content: ABH, AM. Final approval of the article: ABH, HZ, VGBB, LC, JL, KF, AM. Provision of study materials or patients: ABH, AM. Statistical expertise: ABH, VGBB, AM. Obtaining of funding: ABH, AM. Administrative, technical, or logistic support: ABH, AM. Collection and assembly of data: ABH, HZ, LC, JL, KF.

Role of the funding source

Research reported in this publication was supported by the National Institute of Arthritis and Musculoskeletal and Skin Diseases of the National Institutes of Health under Award Numbers R01 AR075730 (to A.M.) and F31 AR082294 (to A.B.). Support for histology was provided by the Washington University Musculoskeletal Research Center (NIH P30 AR074992). Histology slides were imaged with the Nanozoomer at Alafi Neuroimaging Core at Washington University (S10 RR027552). The content is solely the responsibility of the authors and does not necessarily represent the official views of the National Institutes of Health.

Conflict of Interests

All authors declare that they have no conflicts of interest.

Acknowledgements

We would like to thank the Cores and Staff of the Washington University Musculoskeletal Research Center for their assistance. Specifically, thanks to Crystal Idleburg and Samantha Coleman for histological processing and sectioning. We would also like to thank our orthopaedic surgeon collaborators, Kimberly Bartosiak, MD, Ilya Bendich, MD, MBA, and Charles Hannon, MD, MBA, for providing cartilage tissues used to isolate cartilage progenitor cells. We would also like to thank Brian DeBosch, Cassie Higgins, Harrison Gabel and Ladan Abbasi for their generous tissue section donations for use in AQP9 antibody validation.

Appendix A. Supplementary data

Supplementary data to this article can be found online at https://doi.org/10.1016/j.ocarto.2024.100550.

References

[1] D. Chen, J. Shen, W. Zhao, T. Wang, L. Han, J.L. Hamilton, H.J. Im, Osteoarthritis: toward a comprehensive understanding of pathological mechanism, Bone Research 5 (2017) 16044, https://doi.org/10.1038/boneres.2016.44.
[2] A. McAlinden, G.I. Im, MicroRNAs in orthopaedic research: disease associations, potential therapeutic applications, and perspectives, Journal of Orthopaedic Research 36 (1) (2018) 33–51, https://doi.org/10.1002/jor.23822.
[3] A.P. Hensley, A. McAlinden, The role of microRNAs in bone development, Bone 143 (2021) 115760, https://doi.org/10.1016/j.bone.2020.115760.
[4] A. McAlinden, N. Varghese, L. Wirthlin, L.W. Chang, Differentially expressed microRNAs in chondrocytes from distinct regions of developing human cartilage, PLoS One 8 (9) (2013) e75012, https://doi.org/10.1371/journal.pone.0075012.
[5] Z. Yang, X. Wan, Z. Gu, H. Zhang, X. Yang, L. He, R. Miao, Y. Zhong, H. Zhao, Evolution of the mir-181 microRNA family, Computers in Biology and Medicine 52 (2014) 82–87, https://doi.org/10.1016/j.compbiomed.2014.06.004.
[6] A. Bell-Hensley, S. Das, A. McAlinden, The miR-181 family: wide-ranging pathophysiological effects on cell fate and function, Journal of Cellular Physiology 238 (4) (2023) 698–713, https://doi.org/10.1002/jcp.30969.
[7] H. Zheng, J. Liu, E. Tycksen, R. Nunley, A. McAlinden, MicroRNA-181a/b-1 over-expression enhances osteogenesis by modulating PTEN/PI3K/AKT signaling and mitochondrial metabolism, Bone 123 (2019) 92–102, https://doi.org/10.1016/j.bone.2019.03.020.
[8] A. Nakamura, Y.R. Rampersaud, A. Sharma, S.J. Lewis, B. Wu, P. Datta, K. Sundararajan, H. Endisha, E. Rossomacha, J.S. Rockel, I. Jurisica, M. Kapoor, Identification of microRNA-181a-5p and microRNA-4454 as mediators of facet cartilage degeneration, JCI Insight 1 (12) (2016) e86820, https://doi.org/10.1172/jci.insight.86820.
[9] A. Nakamura, Y.R. Rampersaud, S. Nakamura, A. Sharma, F. Zeng, E. Rossomacha, S.A. Ali, R. Krawetz, N. Haroon, A.V. Perruccio, N.N. Mahomed, R. Gandhi, J.S. Rockel, M. Kapoor, microRNA-181a-5p antisense oligonucleotides attenuate osteoarthritis in facet and knee joints, Annals of the Rheumatic Diseases 78 (1) (2019) 111–121, https://doi.org/10.1136/annrheumdis-2018-213629.
[10] G.P. Dowthwaite, J.C. Bishop, S.N. Redman, I.M. Khan, P. Rooney, D.J. Evans, L. Haughton, Z. Bayram, S. Boyer, B. Thomson, M.S. Wolfe, C.W. Archer, The surface of articular cartilage contains a progenitor cell population, Journal of Cell Science 117 (Pt 6) (2004) 889–897, https://doi.org/10.1242/jcs.00912.
[11] A. Bell-Hensley, H. Zheng, A. McAlinden, Modulation of MicroRNA expression during in vitro chondrogenesis, Methods in Molecular Biology 2598 (2023) 197–215, https://doi.org/10.1007/978-1-0716-2839-3_15.
[12] A.S. Yoo, A.X. Sun, L. Li, A. Shcheglovitov, T. Portmann, Y. Li, C. Lee-Messer, R.E. Dolmetsch, R.W. Tsien, G.R. Crabtree, MicroRNA-mediated conversion of human fibroblasts to neurons, Nature 476 (7359) (2011) 228–231, https://doi.org/10.1038/nature10323.
[13] B.D. Markway, H. Cho, B. Johnstone, Hypoxia promotes redifferentiation and suppresses markers of hypertrophy and degeneration in both healthy and osteoarthritic chondrocytes, Arthritis Research and Therapy 15 (4) (2013) R92, https://doi.org/10.1186/ar4272.
[14] A. Oganesian, Y. Zhu, L.J. Sandell, Type IIA procollagen amino propeptide is localized in human embryonic tissues, Journal of Histochemistry and Cytochemistry 45 (11) (1997) 1469–1480, https://doi.org/10.1177/002215549704501104.
[15] M. Amiry-Moghaddam, H. Lindland, S. Zelenin, B.A. Roberg, B.B. Gundersen, P. Petersen, E. Rinvik, I.A. Torgner, O.P. Ottersen, Brain mitochondria contain aquaporin water channels: evidence for the expression of a short AQP9 isoform in the inner mitochondrial membrane, FASEB Journal 19 (11) (2005) 1459–1467, https://doi.org/10.1096/fj.04-3515com.
[16] A. Dobin, C.A. Davis, F. Schlesinger, J. Drenkow, C. Zaleski, S. Jha, P. Batut, M. Chaisson, T.R. Gingeras, STAR: ultrafast universal RNA-seq aligner, Bioinformatics 29 (1) (2013) 15–21, https://doi.org/10.1093/bioinformatics/bts635.
[17] Y. Liao, G.K. Smyth, W. Shi, featureCounts: an efficient general purpose program for assigning sequence reads to genomic features, Bioinformatics 30 (7) (2014) 923–930, https://doi.org/10.1093/bioinformatics/btt656.
[18] M.D. Robinson, D.J. McCarthy, G.K. Smyth, edgeR: a Bioconductor package for differential expression analysis of digital gene expression data, Bioinformatics 26 (1) (2010) 139–140, https://doi.org/10.1093/bioinformatics/btp616.
[19] M.E. Ritchie, B. Phipson, D. Wu, Y. Hu, C.W. Law, W. Shi, G.K. Smyth, Limma powers differential expression analyses for RNA-sequencing and microarray studies, Nucleic Acids Research 43 (7) (2015) e47, https://doi.org/10.1093/nar/gkv007.
[20] R. Liu, A.Z. Holik, S. Su, N. Jansz, K. Chen, H.S. Leong, M.E. Blewitt, M.L. Asselin-Labat, G.K. Smyth, M.E. Ritchie, Why weight? Modelling sample and observational level variability improves power in RNA-seq analyses, Nucleic Acids Research 43 (15) (2015) e97, https://doi.org/10.1093/nar/gkv412.
[21] W. Luo, M.S. Friedman, K. Shedden, K.D. Hankenson, P.J. Woolf, GAGE: generally applicable gene set enrichment for pathway analysis, BMC Bioinformatics 10 (2009) 161, https://doi.org/10.1186/1471-2105-10-161.
[22] V. Agarwal, G.W. Bell, J.W. Nam, D.P. Bartel, Predicting effective microRNA target sites in mammalian mRNAs, Elife 4 (2015), https://doi.org/10.7554/eLife.05005.
[23] B. John, A.J. Enright, A. Aravin, T. Tuschl, C. Sander, D.S. Marks, Human MicroRNA targets, PLoS Biology 2 (11) (2004) e363, https://doi.org/10.1371/journal.pbio.0020363.
[24] J. Zhu, F.L. Wang, H.B. Wang, N. Dong, X.M. Zhu, Y. Wu, Y.T. Wang, Y.M. Yao, TNF-alpha mRNA is negatively regulated by microRNA-181a-5p in maturation of dendritic cells induced by high mobility group box-1 protein, Scientific Reports 7 (1) (2017) 12239, https://doi.org/10.1038/s41598-017-12492-3.
[25] L.J. Sandell, A.M. Nalin, R.A. Reife, Alternative splice form of type II procollagen mRNA (IIA) is predominant in skeletal precursors and non-cartilaginous tissues during early mouse development, Developmental Dynamics 199 (2) (1994) 129–140, https://doi.org/10.1002/aja.1001990206.
[26] A. O'Loghlen, A.M. Munoz-Cabello, A. Gaspar-Maia, H.A. Wu, A. Banito, N. Kunowska, T. Racek, H.N. Pemberton, P. Beolchi, F. Lavial, O. Masui, M. Vermeulen, T. Carroll, J. Graumann, E. Heard, N. Dillon, V. Azuara, A.P. Snijders, G. Peters, E. Bernstein, J. Gil, MicroRNA regulation of Cbx7 mediates a switch of Polycomb orthologs during ESC differentiation, Cell Stem Cell 10 (1) (2012) 33–46, https://doi.org/10.1016/j.stem.2011.12.004.
[27] J.Q. Zhang, B.W. Gao, H.X. Guo, Q.L. Ren, X.W. Wang, J.F. Chen, J. Wang, Z.J. Zhang, Q. Ma, B.S. Xing, miR-181a promotes porcine granulosa cell apoptosis by targeting TGFBR1 via the activin signaling pathway, Molecular and Cellular Endocrinology 499 (2020) 110603, https://doi.org/10.1016/j.mce.2019.110603.
[28] R.M. Marin, J. Vanicek, Efficient use of accessibility in microRNA target prediction, Nucleic Acids Research 39 (1) (2011) 19–29, https://doi.org/10.1093/nar/gkq768.
[29] N.P.T. Huynh, B. Zhang, F. Guilak, High-depth transcriptomic profiling reveals the temporal gene signature of human mesenchymal stem cells during chondrogenesis, FASEB Journal 33 (1) (2019) 358–372, https://doi.org/10.1096/fj.201800534R.
[30] J.M. Carbrey, D.A. Gorelick-Feldman, D. Kozono, J. Praetorius, S. Nielsen, P. Agre, Aquaglyceroporin AQP9: solute permeation and metabolic control of expression in liver, Proceedings of the National Academy of Sciences of the United States of America 100 (5) (2003) 2945–2950, https://doi.org/10.1073/pnas.0437994100.
[31] D.E. Anderson, B.D. Markway, K.J. Weekes, H.E. McCarthy, B. Johnstone, Physioxia promotes the articular chondrocyte-like phenotype in human chondroprogenitor-derived self-organized tissue, Tissue Engineering Part A 24 (3–4) (2018) 264–274, https://doi.org/10.1089/ten.TEA.2016.0510.
[32] G. Pattappa, B.D. Markway, D. Docheva, B. Johnstone, Physioxic culture of chondrogenic cells, Methods in Molecular Biology 2598 (2023) 45–63, https://doi.org/10.1007/978-1-0716-2839-3_5.
[33] J. Heinonen, H. Taipaleenmaki, P. Roering, M. Takatalo, L. Harkness, J. Sandholm, H. Uusitalo-Jarvinen, M. Kassem, I. Kiviranta, T. Laitala-Leinonen, A.M. Saamanen, Snorc is a novel cartilage specific small membrane proteoglycan expressed in differentiating and articular chondrocytes, Osteoarthritis and Cartilage 19 (8) (2011) 1026–1035, https://doi.org/10.1016/j.joca.2011.04.016.
[34] G. Groma, I. Grskovic, S. Schael, H.W. Ehlen, R. Wagener, A. Fosang, A. Aszodi, M. Paulsson, B. Brachvogel, F. Zaucke, Matrilin-4 is processed by ADAMTS-5 in late Golgi vesicles present in growth plate chondrocytes of defined differentiation state, Matrix Biology 30 (4) (2011) 275–280, https://doi.org/10.1016/j.matbio.2011.04.002.
[35] I.M. Shapiro, K. Debolt, V.L. Funanage, S.M. Smith, R.S. Tuan, Developmental regulation of creatine kinase activity in cells of the epiphyseal growth cartilage, Journal of Bone and Mineral Research : the Official Journal of the American Society for Bone and Mineral Research 7 (5) (1992) 493–500, https://doi.org/10.1002/jbmr.5650070505.
[36] J. Henao-Mejia, A. Williams, L.A. Goff, M. Staron, P. Licona-Limon, S.M. Kaech, M. Nakayama, J.L. Rinn, R.A. Flavell, The microRNA miR-181 is a critical cellular metabolic rheostat essential for NKT cell ontogenesis and lymphocyte development and homeostasis, Immunity 38 (5) (2013) 984–997, https://doi.org/10.1016/j.immuni.2013.02.021.
[37] H. Zhao, Y. Guo, Y. Sun, N. Zhang, X. Wang, miR-181a/b-5p ameliorates inflammatory response in monocrotaline-induced pulmonary arterial hypertension by targeting endocan, Journal of Cellular Physiology 235 (5) (2020) 4422–4433, https://doi.org/10.1002/jcp.29318.
[38] N.P. Huynh, C.C. Gloss, J. Lorentz, R. Tang, J.M. Brunger, A. McAlinden, B. Zhang, F. Guilak, Long non-coding RNA GRASLND enhances chondrogenesis via suppression of the interferon type II signaling pathway, Elife 9 (2020), https://doi.org/10.7554/eLife.49558.

[39] D. Wang, Y. Fang, L. Lin, W. Long, L. Wang, L. Yu, H. Deng, D. Wang, Upregulating miR-181b promotes ferroptosis in osteoarthritic chondrocytes by inhibiting SLC7A11, BMC Musculoskelet Disorder 24 (1) (2023) 862, https://doi.org/10.1186/s12891-023-07003-7.

[40] D. Zhao, Y. Li, Y. Li, Z. Jiang, D. Shen, Z. Zhao, F. Wang, MiR-181a regulates the chondrogenic differentiation in pig peripheral blood mesenchymal stem cells, International Journal of Clinical and Experimental Pathology 11 (2) (2018) 947–955.

[41] J. Gabler, M. Ruetze, K.L. Kynast, T. Grossner, S. Diederichs, W. Richter, Stage-specific miRs in chondrocyte maturation: differentiation-dependent and hypertrophy-related miR clusters and the miR-181 family, Tissue Engineering Part A 21 (23–24) (2015) 2840–2851, https://doi.org/10.1089/ten.TEA.2015.0352.

[42] A.K. Azad, T. Raihan, J. Ahmed, A. Hakim, T.H. Emon, P.A. Chowdhury, Human aquaporins: functional diversity and potential roles in infectious and non-infectious diseases, Frontiers in Genetics 12 (2021) 654865, https://doi.org/10.3389/fgene.2021.654865.

[43] I.V. da Silva, S. Garra, G. Calamita, G. Soveral, The multifaceted role of aquaporin-9 in Health and its potential as a clinical biomarker, Biomolecules 12 (7) (2022), https://doi.org/10.3390/biom12070897.

[44] K. Takeuchi, S. Hayashi, T. Matumoto, S. Hashimoto, K. Takayama, N. Chinzei, S. Kihara, M. Haneda, S. Kirizuki, Y. Kuroda, M. Tsubosaka, K. Nishida, R. Kuroda, Downregulation of aquaporin 9 decreases catabolic factor expression through nuclear factor-kappaB signaling in chondrocytes, International Journal of Molecular Medicine 42 (3) (2018) 1548–1558, https://doi.org/10.3892/ijmm.2018.3729.

[45] R.B. Gletten, L.S. Cantrell, S. Bhattacharya, K.L. Schey, Lens aquaporin-5 inserts into bovine fiber cell plasma membranes via unconventional protein secretion, Investigative Ophthalmology & Visual Science 63 (8) (2022) 5, https://doi.org/10.1167/iovs.63.8.5.

[46] S. Bestetti, M. Galli, I. Sorrentino, P. Pinton, A. Rimessi, R. Sitia, I. Medrano-Fernandez, Human aquaporin-11 guarantees efficient transport of H(2)O(2) across the endoplasmic reticulum membrane, Redox Biology 28 (2020) 101326, https://doi.org/10.1016/j.redox.2019.101326.

[47] R. Aharon, Z. Bar-Shavit, Involvement of aquaporin 9 in osteoclast differentiation, The Journal of Biological Chemistry 281 (28) (2006) 19305–19309, https://doi.org/10.1074/jbc.M601728200.

[48] Y. Liu, L. Song, Y. Wang, A. Rojek, S. Nielsen, P. Agre, J.M. Carbrey, Osteoclast differentiation and function in aquaglyceroporin AQP9-null mice, Cell Biology 101 (3) (2009) 133–140, https://doi.org/10.1042/BC20080083.

[49] G. Bu, F. Shuang, Y. Wu, D. Ren, S. Hou, AQP9: a novel target for bone loss induced by microgravity, Biochemical and Biophysical Research Communications 419 (4) (2012) 774–778, https://doi.org/10.1016/j.bbrc.2012.02.100.

[50] P. Tang, Characterizing AQP9: A Regulator of Epiphyseal Plate Chondrocyte Proliferation, Hypertrophy, and Long Bone Growth, Institute of Medical Science University of Toronto, Toronto, CA, 2018, p. 159.